

DOI: 10.17725/rensit.2023.15.003

## Magnetoimpedance in a Planar Magnetolectric Heterostructure Amorphous Ferromagnet–Piezoelectric: Electric Field Modulation

Dmitri A. Burdin, Dmitri V. Chashin, Nikolai A. Ekonomov, Yuri K. Fetisov

MIREA–Russian Technological University, <http://www.mirea.ru/>

Moscow 119454, Russian Federation

*E-mail: burdin@mirea.ru; chashin@mirea.ru; ekonomov@list.ru; fetisov@mirea.ru*

Peng Zhou, Yajun Qi, Tianjin Zhang

Hubei University, <https://eng.hubu.edu.cn/>

Wuhan 430062, PR China

*E-mail: p\_zhou@outlook.com, yajun\_qi@hotmail.com, zhangtj@hubu.edu.cn*

Larissa V. Panina

University of Science and Technologies MISIS, <https://misis.ru/>

Moscow 119049, Russian Federation

*E-mail: drlpanina@gmail.com*

*Received January 04, 2023, peer-reviewed January 06, 2023, accepted January 09, 2023*

**Abstract:** The magnetoimpedance effect and the converse magnetolectric effect in a planar heterostructure consisting of mechanically bonded layers of amorphous ferromagnet FeBSiC and piezoelectric lead zirconate titanate are studied. Magnetoimpedance was observed in the frequency range of 0.1-40 MHz and bias dc magnetic field of 0-300 Oe; the maximum magnitude of the effect at a frequency of 10 MHz reached 12%. The converse magnetolectric effect was observed in magnetic fields of 0-50 Oe; the maximum value of the effect at the structure acoustic resonance frequency of 40 kHz was 1.45 G/(V/cm). Amplitude modulation of the magnetoimpedance by an electric field at the resonance frequency of the structure with a coefficient of  $\sim 1 \cdot 10^{-2}$  is found. Modulation occurs as a result of a combination of the piezoelectricity and magnetostriction of the layers, which leads to a change in the transverse magnetic permeability and the thickness of the skin-layer of the ferromagnet.

**Keywords:** magnetoimpedance, composite heterostructure, ferromagnet, piezoelectric, magnetolectric effect

**UDC 537.86**

**Acknowledgments:** The work was supported by Russian Fund for Fundamental Research, grants 20-07-00811 (experiment) and 20-31-70001 (theoretical analysis). Some measurements were carried out on the equipment of the Joint Center for Common Use of RTU MIREA.

**For citation:** Dmitri A. Burdin, Dmitri V. Chashin, Nikolai A. Ekonomov, Peng Zhou, Yajun Qi, Tianjin Zhang, Larissa V. Panina, Yuri K. Fetisov. Magnetoimpedance in a Planar Magnetolectric Heterostructure Amorphous Ferromagnet–Piezoelectric: Electric Field Modulation. *RENSIT: Radioelectronics. Nanosystems. Information Technologies*, 2023, 15(1):3-12e. DOI: 10.17725/rensit.2023.15.003.

### CONTENTS

1. INTRODUCTION (4)

2. HETEROSTRUCTURE AND MEASUREMENT TECHNIQUES (5)

3. CHARACTERISTICS OF MAGNETOIMPEDANCE (6)

4. ELECTRIC FIELD EFFECT ON THE STRUCTURE CHARACTERISTICS (6)

**A. CONVERSE ME EFFECT (6)****B. MODULATION OF MAGNETOIMPEDANCE (7)****5. RESULTS DISCUSSION (8)****6. CONCLUSION (10)****REFERENCES (10)****1. INTRODUCTION**

The magnetoimpedance (MI) effect in magnetic conductors has been intensively studied in recent decades in connections with the prospects for its use in magnetic field sensors [1]. The effect manifests itself in a change in the impedance of the sample under the action of a dc magnetic field and arises due to a change in the magnetic permeability with a subsequent change in the thickness of the skin-layer in the conductor [2,3]. In iron and cobalt based amorphous ferromagnets, the field-induced change in impedance reaches hundreds of percent and strongly depends on the composition and geometry of the samples, as well as on external conditions [4]. In magnetostrictive materials, the sample deformation (stress-impedance effect) can influence the magnetization direction and magnetic permeability  $\mu$  of the material, therefore, can also lead [5-6] to the impedance change.

It is of interest to explore the possibility of controlling MI effect with the help of dynamic deformations. For this, composite heterostructures consisting of mechanically coupled ferromagnetic (FM) and piezoelectric (PE) layers can be used. In such heterostructures, magnetoelectric (ME) effects are observed, which arise as a result of a combination of piezoelectricity in the PE layer and magnetostriction of the FM layer, leading to a change in the magnetization  $M$  or electric polarization  $P$  of the structure under

the action of magnetic  $H$  and electric  $E$  fields [7,8].

To date, several articles devoted to the study of MI effects in composite heterostructures have been published. In a ring resonator with ceramic layers made of lead zirconate titanate (PZT) and ferromagnetic Terfenol a change in the capacitive component of the impedance by 225% was observed under the action of a magnetic field of 800 mT at the acoustic resonance frequency of 70 kHz [9]. In the structure of an amorphous ferromagnet Metglas-PZT at a resonance frequency of 60 kHz, a change in the inductive and capacitive components of the impedance up to 450% in a magnetic field of 100 Oe was found [10]. In [11], the MI effect in the Metglas-PZT and Terfenol-PZT structures was studied and it was shown that magnitude of the impedance significantly depends on the magnetic and dielectric permittivities, magnetostriction, and Young's moduli of the structure layers. In the Metglas-PZT structure, the impedance change of 600% was registered, which is an order of magnitude greater than in the Terfenol-PZT structure.

In this work we studied the MI effect in the Metglas-PZT planar heterostructure and demonstrated for the first time the possibilities of controlling the magnetoimpedance using an electric field applied to the piezoelectric layer of the structure.

The first part of the article contains a description of the structure under study and measurement techniques. The second part presents the measured magnetoimpedance characteristics of the structure. The third part is devoted to the study of the electric field effect on the characteristics of the structure. In the last part, the results obtained are discussed.

The conclusion summarizes main results of the research.

2. HETEROSTRUCTURE AND MEASUREMENT TECHNIQUES

The heterostructure under study and the block-diagram of the measuring setup are shown schematically in Fig. 1. The structure contained ferromagnetic and piezoelectric layers. The FM layer was made of an amorphous ferromagnetic FeBSiC foil (Metglas 2605SA1, Metglas Inc., USA), with planar dimensions of 23×1.7 mm and thickness of 25 μm. The physical parameters are: the saturation magnetization  $M_s = 1.56$  T, relative magnetic permeability  $\mu \sim 10^4$ , saturation magnetostriction  $\lambda_s = 25 \cdot 10^{-6}$ , and specific conductivity  $\sigma \approx 8.3 \cdot 10^5 \Omega^{-1}m^{-1}$ . The PE plate was made of lead zirconate-titanate piezoceramic of the composition  $Pb_xZr_{1-x}TiO_3$  (PZT-43, JSC Elpa Research Institute, Moscow, Russia), with the dimensions of 81.3×12×3 mm. The physical parameters are: the piezoelectric modules  $d_{33} = 280$  pm/V and  $d_{31} = -125$  pm/V, the relative dielectric constant  $\epsilon = 1400$ . A part of the PZT plate, 40 mm long with Ag-electrodes

on the surface, was electrically poled along the normal to the plane, while the free part was poled in the plane of the plate. The Metglas strip was bonded to the free part of the PZT plate using cyanoacrylate adhesive. The thick adhesive layer (~10 μm) effectively transmitted deformations through the interface and provided electrical isolation of the Metglas conductive strip from the PZT plate. The structure was placed between the poles of an electromagnet generating a dc magnetic field  $H$  up to 0-400 Oe applied along its long axis. The magnetic field was measured with a gaussmeter (LakeShore, model 421) with an accuracy of 0.1 Oe.

When studying the magnetoimpedance, an ac current with an amplitude  $I = 20-200$  mA and a frequency  $f = 0.1-40$  MHz from an Agilent 33611A generator was passed through the Metglas strip. The voltage  $u$  between the ends of the FM strip was measured with a lock-in amplifier Stanford Research SR844. The absolute value of the impedance was determined as the ratio of the voltage and current amplitudes  $Z = u/I$  and the MI ratio as a function of the field  $H$  was calculated in a standard way:

$$MI(H) = \frac{Z(H) - Z(H_s)}{Z(H_s)} 100\%, \tag{1}$$

where  $Z(H_s)$  is the impedance at the saturation field  $H_s$ . The frequency spectrum of the magnetoimpedance voltage across the Metglas strip was measured using a Siglent SSA3021X spectrum analyzer

When studying the electric field influence on the structure characteristics, an ac voltage with an amplitude up to  $U = 10$  V and frequency  $F = 10$  Hz – 100 kHz from the second Agilent 33210A generator was applied to the electrodes of the PZT layer. This voltage produced an ac electric field with an amplitude up to  $e = 33$  V/cm

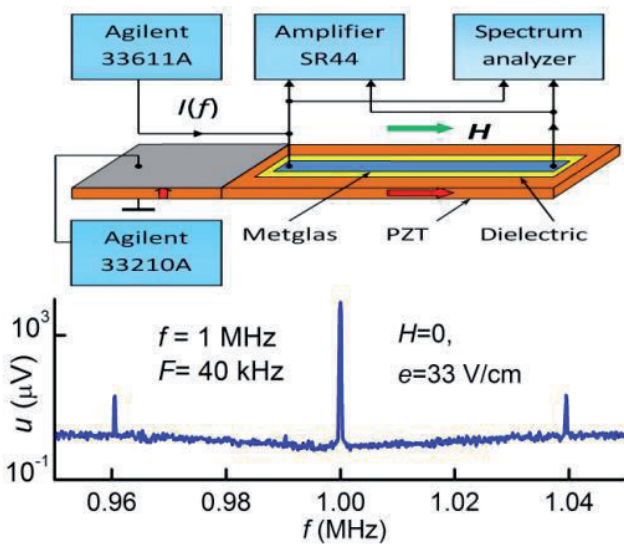


Fig. 1. Block-diagram of the Metglas-PZT heterostructure and measurement setup. Arrows indicate directions of electric and magnetic fields.

in the piezoelectric layer. The change in the magnetization of the structure was measured using a coil of 30 mm in diameter with  $N = 270$  turns wound around the structure. All measurements were carried out at room temperature.

### 3. CHARACTERISTICS OF MAGNETOIMPEDANCE

At the first stage, the MI characteristics of the structure in the absence of electric field were studied. At  $H = 0$ , and a frequency  $f = 10$  MHz, the maximum of the voltage drop across the strip  $u \approx 13.7$  mV was measured giving the value of  $Z(0) \approx 0.685 \Omega$ .

**Fig. 2** shows the MI ratio of the Metglas strip vs. magnetic field  $H$  for various current frequencies and  $I = 20$  mA. It is seen that the width of the magnetoimpedance field region strongly depends on the current frequency. For the saturation magnetic field  $H_s \approx 350$  Oe, the impedance was  $Z(H_s) \approx 0.61 \Omega$  and the maximum of the MI ratio was about 12%. For frequencies below 20 MHz, the impedance plots have a central peak at  $H = 0$ . For higher frequencies, a dip appears near the zero field, which becomes more pronounced with increasing

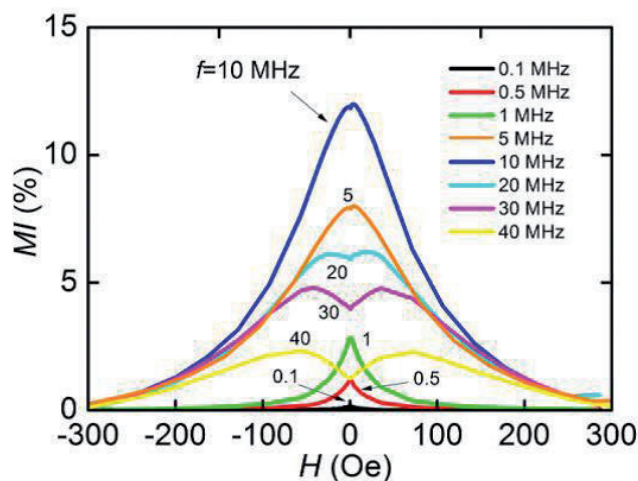


**Fig. 2.** MI ratio in the Metglas-PZT structure as a function of magnetic field  $H$  for various frequencies  $f$ .

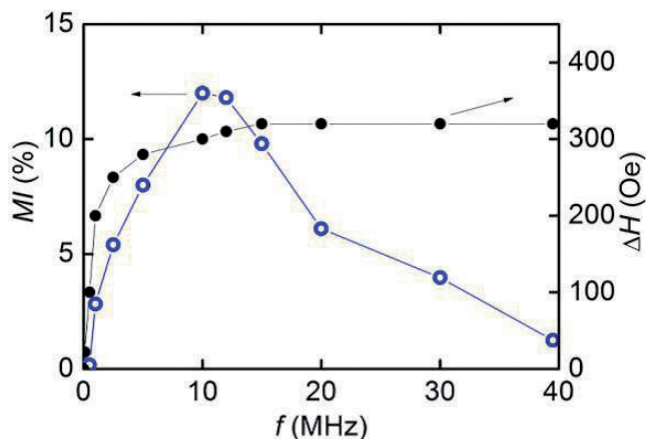


**Fig. 3.** MI ratio at  $H = 0$  and width of the magnetoimpedance field region  $\Delta H$  in the Metglas-PZT structure as a function of frequency  $f$ .

frequency. For all frequencies, the MI plots are hysteresis-free.

**Fig. 3** compares the MI ratio at zero field for different frequencies along with the range of magnetic fields  $\Delta H$  affecting the impedance. For low frequencies, the MI ratio is small due to a weak skin-effect, the saturation field and  $\Delta H$  are also small. For current frequencies above 1 MHz, the  $\Delta H$  expands from 100 to  $\sim 330$  Oe with increasing  $f$ . For frequencies higher than 10 MHz, the MI ratio at zero field decreases as the shape of the MI plots changes. The shapes of the plots of  $MI(H)$  and  $MI(f)$  shown in Figs. 2, 3 and the MI maximum of 12% in the Metglas strip are consistent with the data of other studies of magnetoimpedance in amorphous ferromagnetic strips [1,12].

### 4. ELECTRIC FIELD EFFECT ON THE STRUCTURE CHARACTERISTICS

At the second stage, we studied the effect of an ac electric field  $e \cos(2\pi Ft)$  applied to the PZT layer on the characteristics of the structure. The electric field leads to the modulation of the magnetization of the structure (converse ME effect) [13], and to the modulation of its magnetoimpedance.

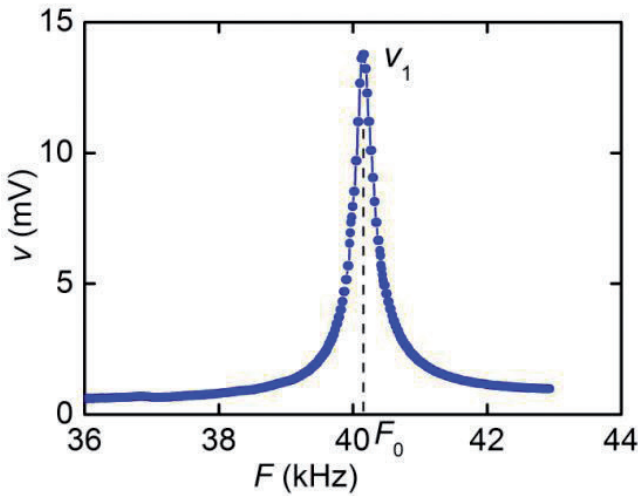


**Fig. 4.** Dependence of voltage from the coil  $v$  on the frequency of electric field  $F$  for the converse ME effect in the Metglas-PZT structure at  $H \approx 4.2$  Oe and  $e = 33$  V/cm.

**A. CONVERSE ME EFFECT**

**Fig. 4** shows the dependence of the voltage  $v$  from the coil on the frequency  $F$  of the electric field for  $e = 33$  V/cm. The voltage peak near the frequency  $F_0 = 40.15$  kHz with amplitude  $v_1 = 13.8$  mV and quality factor  $Q \approx 48$  corresponds to the excitation of longitudinal acoustic oscillations in the structure (as will be shown below).

**Fig. 5** presents the dependence of the voltage  $v_1$  from the coil on the magnetic field  $H$ . It can be seen, that the voltage

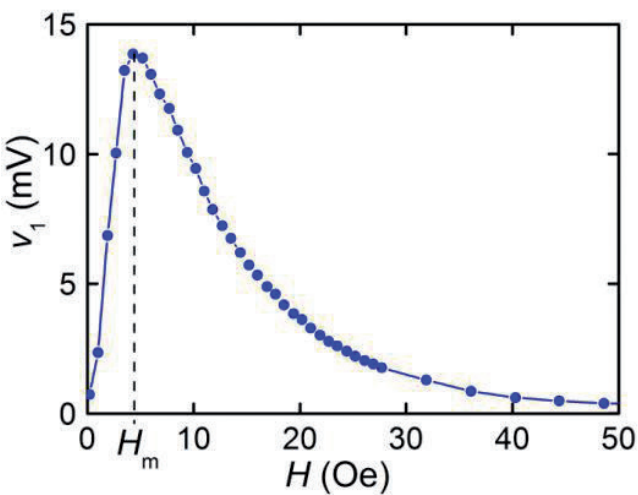


**Fig. 5.** Dependence of the voltage from the coil  $v_1$  on the magnetic field  $H$  for the converse ME effect in the Metglas-PZT structure at  $e = 33$  V/cm.

initially increases with increasing  $H$ , reaches a maximum at a field  $H_m \approx 4.2$  Oe, and then drops to zero as the FM layer is saturated. The field  $H_m$  corresponds to the maximum of the piezomagnetic coefficient  $\lambda^{(1)}(H) = \partial\lambda/\partial H|_{HP}$ , where  $\lambda(H)$  is the Metglas magnetostriction as a function of the field. As can be seen from Fig. 5, the converse ME effect in the described structure is observed in the region of magnetic fields of 0-50 Oe.

**B. MODULATION OF MAGNETOIMPEDANCE**

Modulation of the magnetoimpedance of the structure under the action of ac electric field was observed through the frequency spectra of the voltage across the Metglas strip. As an example, **Fig. 6** shows the voltage spectra for current frequency  $f = 1$  MHz, amplitude 20 mA, and  $H = 0$ . It can be seen that in the absence of electric field ( $e = 0$ ), the voltage spectrum contains only one component with the frequency of 1 MHz, which is equal to the current frequency (fundamental harmonic). AC field with an amplitude  $e = 33$  V/cm and a frequency  $F = 39.5$  kHz results in the appearance of side components with an amplitude  $u_s$  and combination frequencies in the voltage spectrum. Amplitudes of the

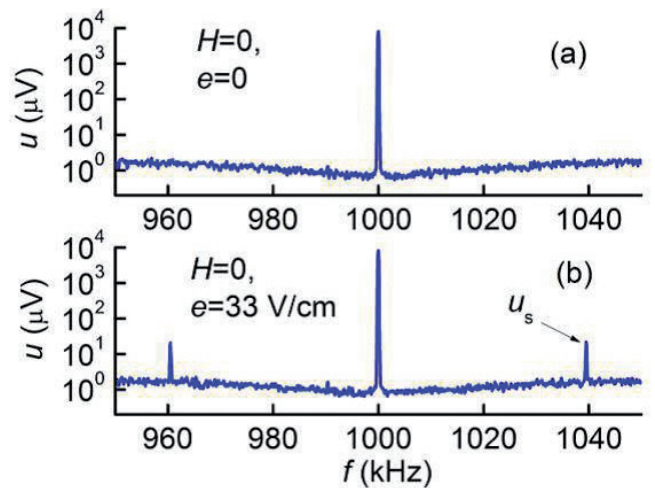


**Fig. 6.** Frequency spectrum of MI voltage: (a) in the absence of an electric field, (b) when a field  $e = 33$  V/cm with a frequency  $F = 39.5$  kHz is applied to the PZT layer.

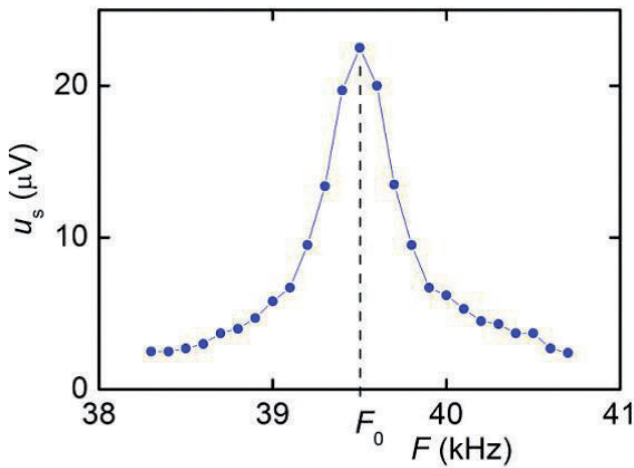


**Fig. 7.** Dependence of the side component amplitude  $u_s$  of the MI voltage spectrum on the frequency of the electric field  $F$  at  $e = 33 \text{ V/cm}$  and  $H = 0$ .

side components are  $\sim 10 \text{ dB}$  higher than the noise level.

**Fig. 7** shows the dependence of the side components amplitude  $u_s$  on the electric field frequency  $F$ . The amplitude reaches a maximum of  $22 \text{ mV}$  at the resonance frequency of the structure  $F_0$ , the line has a quality factor  $Q \approx 116$ . The amplitude of the side components  $u_s$  linearly increased with the field amplitude  $e$  and decreased monotonically with increasing  $H$ .

**Fig. 8** shows the dependence of the amplitude  $u_s$  of the side components on

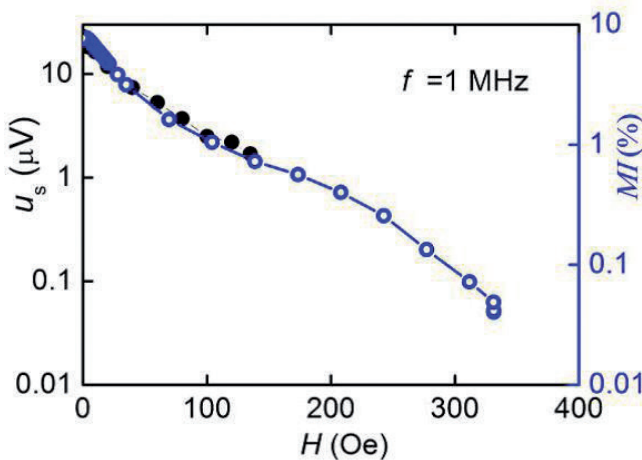


**Fig. 8.** Dependences of the side component amplitude  $u_s$  of the MI voltage spectrum (solid circles) and MI ratio (open circles) on the field  $H$  at the resonance frequency  $F_0$ . Logarithmic scale is used on vertical axis.

the field  $H$  at the resonant frequency for  $f = 1 \text{ MHz}$  and  $e = 33 \text{ V/cm}$ . For comparison, the field dependence of the  $MI(H)$  ratio is also presented. The two curves can be superimposed on each other. The harmonics with combination frequencies in the signal spectrum with  $f = 1 \text{ MHz}$  were observed in the field range from zero to  $\sim 135 \text{ Oe}$ , and in the signal spectrum with  $f = 10 \text{ MHz}$ , in the field range from zero to  $\sim 330 \text{ Oe}$ .

The measurements described above were also carried out using a structure with FM layer of amorphous ferromagnetic alloy having magnetostriction  $\lambda_s < 1 \cdot 10^{-6}$ . In such a structure, a magnetoimpedance was observed, but the ME effect and MI modulation by an electric field were absent.

## 5. RESULTS DISCUSSION

Let us consider in more detail the mechanisms of the converse ME effect and the modulation of the impedance by the electric field in the described structure.

The converse ME effect in the structure arises due to the combination of the inverse piezoelectric effect in the PZT layer and the inverse magnetostriction (Villari effect) in the Metglas strip due to the mechanical coupling of the layers [7]. An ac field  $e$  produces a deformation of the PZT layer, this deformation is transferred to the Metglas strip, which leads to modulation of its magnetization  $M$  and permeability.

First, we estimate the resonant frequency of the structure (Fig. 4) using the formula for the frequency of longitudinal vibrations of a free rod [14]:

$$F_n = \frac{n}{2b} \sqrt{\frac{Y}{\rho}}, \quad (2)$$

where  $b$  is the length of the structure,  $Y$  is the Young modulus,  $\rho$  is the density,  $n = 1, 2, \dots$  is the mode number. Since the thickness and

mass of the Metglas strip and the electrodes are much less than the thickness and mass of the PZT plate, their contribution is not taken into account in the estimation. Using the known PZT parameters ( $Y = 7.7 \cdot 10^{10}$  N/m<sup>2</sup>,  $\rho = 7.5 \cdot 10^3$  kg/m<sup>3</sup>), for a plate of length  $b = 81.3$  mm, we obtain the frequency  $F_n \approx n \cdot 19.7$  kHz. Thus, the frequency of the second mode ( $n = 2$ ) of planar vibrations 39.4 kHz is in a good agreement with the measured resonant frequency. In this case, the Metglas strip is located in the region of the greatest deformations on the surface of the PZT plate.

For the estimation of the ME coefficient for the converse effect, it is necessary to find the amplitude of the induction change  $\delta B$  in the Metglas strip at the resonant frequency. Applying Faraday's law of electromagnetic induction,  $\delta B$  is determined as

$$\delta B = \frac{v}{SN2\pi F_0}, \quad (3)$$

where  $v$  is the voltage from the coil,  $S$  and  $N$  are the cross-section and the number of turns of the coil. The cross section  $S$  should be taken as that of the Metglas strip, because the field is concentrated in the ferromagnet with a large relative permeability  $\mu \sim 10^4$ . Substituting the voltage  $v = 13.8$  mV and the structure parameters, we obtain the change in induction  $\delta B \approx 48$  G. Such variation in  $B$  gives an ME coefficient of  $\alpha_B = \delta B/e \approx 1.45$  G/(V/cm), which agrees in order of magnitude with the coefficients for the FeGa-PZT [15] and Metglas-PZT [16] structures. The relative deformation of the Metglas strip at the resonance frequency under the action of an electric field  $e = 33$  V/cm applied to the structure can be estimated as  $T \approx Qd_{31}e \approx 2 \cdot 10^{-5}$ .

The impedance of a ferromagnetic strip of thickness  $d$ , characterized by the average

transverse permeability (with respect to the current) is of the form [3]:

$$Z = R_{dc} \frac{kd}{2} \cot \frac{kd}{2}, \quad k = \frac{(1+j)}{\delta}. \quad (4)$$

In (4)  $\delta$  is the skin-layer thickness:

$$\delta = \sqrt{\frac{2}{\sigma \omega \mu_0 \mu_t}}, \quad (5)$$

where  $\sigma$  is the conductivity,  $\mu_0$  is the permittivity of vacuum,  $\mu_t$  is the relative transverse permeability of the ferromagnet, which depends on  $H$  and the anisotropy field. The transverse permeability defines the magnetic flux, generated by the field  $b$  created by the current flowing along the FM strip. The value of  $\mu_t$  that enters (4) differs from that found from the magnetization curve  $B(H)$  by differentiation  $\mu(H) = \partial B / \partial H|_H$ . The transverse permeability  $\mu_t$  depends on the bias field  $H$ , the anisotropy field  $H_k$ , and the dimensions of the FM strip [17,18]. In the case of a uniaxial anisotropy, the transverse permeability for frequencies much lower than the ferromagnetic resonance frequency  $\mu_t$  is of the form ( $M_s$  and  $H$  are in CGS units) [19]:

$$\mu_t \approx 1 + \frac{4\pi M_s}{H \cos \theta + H_k \cos 2(\alpha - \theta)}, \quad (6)$$

where  $M_s$  is the saturation magnetization,  $\alpha$  is the angle between the anisotropy axis and current, and  $\theta$  is the angle between the static magnetization and current. If  $\alpha \approx 0$ ,  $\theta \approx 0$ , the value of  $\mu_t$  has a maximum at zero field and decreases as  $1/H$ . This explains the impedance vs. field behaviour at lower frequencies. With  $\mu_t$ -decrease, the skin effect becomes weaker and the change in impedance is not noticeable at higher fields. This explains narrowing of the  $MI$  plots with decreasing frequency  $f$  (see Fig. 3). For higher frequencies, when the skin effect is essential the surface layers of the strip mainly contribute to the impedance. There could be a deviation of the anisotropy axis from the axial

direction. In this case, the permeability has a minimum at zero field what was observed in the impedance behavior at frequencies higher than 20 MHz. For MHz frequencies, the *MI* ratio up to few % was observed for  $H \approx 300$  Oe.

The application of an ac field  $e$  to the PZT layer results in a modulation of the magnetoimpedance. The reason for the occurrence of magnetoimpedance voltage modulation is as follows. As shown in [20], the deformation of FM layer in a heterostructure leads to the appearance of an additional anisotropy field  $H_{me}$  of magnetostrictive origin and directed across the strip axis and perpendicular to  $H$ . Considering that the change in the transverse permeability due to  $H_{me}$  is small, the total permeability is of the form (for  $\alpha \approx 0$ ,  $\theta \approx 0$ )

$$\tilde{\mu}_t = \mu_t \left( 1 + \frac{H_{me}}{H + H_K} \right). \quad (7)$$

Therefore, the field  $H_{me}$  changes the variable component of magnetization (and magnetic induction) in the transverse direction. The magnitude of the magnetic impedance of the strip is modulated with a frequency  $F$  equal to the frequency of the electric field. The induced voltage of the MI signal can be written as

$$u(t) = u_s [(1 + m \cos(2\pi Ft)) \cdot \cos(2\pi ft)]. \quad (8)$$

Here  $m$  is the modulation coefficient, which is related to the amplitude of the central and side components of the spectrum as  $m = 2u_s/u_0$ . Using the data in Fig. 6b and 7, we obtain  $m \approx 10^{-2}$ . Similar field dependences of  $u_s$  and  $MI(H)$  shown in Fig. 6 confirm the *MI* voltage modulation reasoning.

It should be noted the difference in the field dependences of the converse ME effect and MI effect. The ME effect in the considered structure was observed in the range of magnetic fields  $\sim 0-50$  Oe. In the fields above 50 Oe, the Metglas magnetization and

magnetostriction saturate and the magnetic permeability with respect to this field tends to zero. On the other hand, MI effect was observed in a wider range of fields  $\sim 0-330$  Oe, since the impedance depends on the transverse permeability (with respect to current), which describes the change in magnetization due to a field  $b$  generated by the current. Applying a magnetic field  $H$  perpendicular to  $b$  increases the magnetic hardness so the transverse permeability changes as  $1/H$ .

## 6. CONCLUSION

We have studied the magnetoimpedance in a planar heterostructure containing mechanically bonded layers of an amorphous FeBSiC ferromagnet and a piezoelectric PZT. The magnetoimpedance was observed in the frequency range of 0.1-40 MHz and bias fields of 0-300 Oe, the maximum value of the effect at a frequency of 10 MHz reached 12%. It is shown that an ac electric field applied to the piezoelectric layer with a frequency equal to the acoustic resonance frequency of the structure leads to the modulation of the magnetic induction in a ferromagnet (converse ME effect) followed by the modulation of the magnetoimpedance. The field conversion coefficient was 1.45 G/(V/cm), the impedance modulation coefficient reached  $\sim 10^{-2}$ . The modulation occurs as a result of a combination of the piezoelectric effect and magnetostriction of the structure layers, which leads to a change in the magnetic permeability of the ferromagnet. The detected effect can be used to control the parameters of magnetic field sensors.

## REFERENCES

1. Knobel M, Pirota KR. Giant magnetoimpedance: concepts and recent progress. *J. Mag. Magn. Mater.*, 2002, 242-245 (part I):33-40, doi: 10.1016/s0304-8853(01)01180-5.



2. Panina LV, Mohri K. Magneto-impedance effect in amorphous wires. *Appl. Phys. Lett.*, 1994, 65:1189-1191, doi: 10.1063/1.112104.
3. Panina LV, Mohri K, Uchiyama T, Noda M. Giant magneto-impedance in Co-rich amorphous wires and films. *IEEE Trans Magn.*, 1995, 31:1249-1260, doi: 10.1109/20.364815.
4. Phan MH, Peng HX. Giant magnetoimpedance materials: fundamentals and applications, *Progress in Materials Science*, 2008, 53:323-420, doi: 10.1016/j.pmatsci.2007.05.003.
5. Shen LP, Uchiyama T, Mohri K, Kita E, Bushida K. Sensitive Stress-Impedance Micro Sensor Using Amorphous Magnetostrictive Wire. *IEEE Trans. Magn.*, 1997, 33:3355-3357, doi: 10.1109/20.617942.
6. Gazda P, Nowicki M, Szewczyk R. Comparison of stress-impedance effect in amorphous ribbons with positive and negative magnetostriction. *Materials*, 2019, 12:275, doi: 10.3390/ma12020275.
7. Nan CW, Bichurin MI, Dong S, Viehland D, Srinivasan G. Multiferroic magnetolectric composites: Historical perspective, status and future directions. *J. Appl. Phys.*, 2008, 103:031101, doi: 10.1063/1.2836410.
8. Chashin DV, Fetisov YK, Tafintseva EV, Srinivasan G. Magnetolectric effects in layered samples of lead zirconium titanate and nickel films. *Solid State Com.*, 2008, 148:55, doi: 10.1016/j.ssc.2008.07.015.
9. Wang W, Wang Z, Luo X, Tao J, Zhang N, Xu X, Zhou L. Capacitive type magnetoimpedance effect in piezoelectric-magnetostrictive composite resonator. *Appl. Phys. Lett.*, 2015, 107:172904, doi: 10.1063/1.4934821.
10. Leung CM, Zhuang X, Xu J, Li J, Zhang J, Srinivasan G, Viehland D. Enhanced tunability of magneto-impedance and magneto-capacitance in annealed Metglas/PZT magnetolectric composites. *AIP Advances*, 2018, 8:055803, doi: 10.1063/1.5006203.
11. Chen L, Wang Y, Luo T, Zou Y, Wan Z. The Study of Magnetoimpedance Effect for Magnetolectric Laminate Composites with Different Magnetostrictive Layers. *Materials*, 2021, 14:6397, doi: 10.3390/ma14216397.
12. Amalou F, Gijs MAM. Giant magnetoimpedance in trilayer structures of patterned magnetic amorphous ribbons. *Appl. Phys. Lett.*, 2002, 81:1654, doi: 10.1063/1.1499769.
13. Hayes P, Schell V, Salzer S, Burdin D, Yarar E, Piorra A, Knochel R, Fetisov YK, Quqnda E. Electrically modulated magnetolectric AlN/FeCoSiB film composites for DC magnetic field sensing. *J. Phys. D: Appl. Phys.*, 2018, 51:354002, doi: 10.1088/1361-6463/aad456.
14. Timoshenko S. *Vibration Problems in Engineering*. D.Van Nostrand Company Inc., Toronto, 1955, p. 310.
15. Fetisov YK, Kamentsev KE, Chashin DV, Fetisov LY, Srinivasan G. Converse magnetolectric effects in a galfenol and lead zirconate titanate bilayer. *J. Appl. Phys.*, 2009, 105:123918, doi: 10.1063/1.3152953.
16. Fetisov LY, Chashin DV, Burdin DA, Saveliev DV, Ekonomov NA, Srinivasan G, Fetisov YK. Nonlinear converse magnetolectric effects in a ferromagnetic-piezoelectric bilayer. *Appl. Phys. Lett.*, 2018, 113(21):212903, doi: 10.1063/1.5054584.
17. Coisson M, Tiberto P, Vinai F, Tyagi PV, Modak SS, Kane SN. Penetration depth and magnetic permeability calculations on GMI effect and comparison with measurements on CoFeB alloys. *J. Magn. Mag. Mater.*,

- 2008, 320:510-514, doi: 10.1016/j.jmmm.2007.07.010.
18. Franco CS, Ribas GP, Bruno AC. Influence of the anisotropy axis direction and ribbon geometry on the giant magnetoimpedance of Metglas®2705M. *Sensors and Actuators A Physical*, 2006, 132(1):85-89, doi: 10.1016/j.sna.2006.04.047.
19. Makhnovskiy DP, Panina LV, Mapps DJ. Field-dependent surface impedance tensor in amorphous wires with two types of magnetic anisotropy: helical and circumferential. *Phys. Rev.*, 2001, B.63:144424.
20. Yan Y, Geng LD, Zhang L, Gollapudi S, Song HC, Dong S, Sanghadasa M, Ngo K, Priya S. Correlation between tunability and anisotropy in magnetoelectric voltage tunable inductor (VTI). *Scientific Reports*, 2017, 7(1):16008.